2021 43rd Annual International Conference of the
IEEE Engineering in Medicine & Biology Society (EMBC)
Oct 31 - Nov 4, 2021. Virtual Conference

Mapping Functional Connectivity of Epileptogenic Networks through Virtual Implantation

Ludovica Corona, Eleonora Tamilia, Joseph R. Madsen, Steven M. Stufflebeam, Phillip L. Pearl, Christos Papadelis

Abstract — **Children with medically refractory epilepsy (MRE) require resective neurosurgery to achieve seizure freedom, whose success depends on accurate delineation of the epileptogenic zone (EZ). Functional connectivity (FC) can assess the extent of epileptic brain networks since intracranial EEG (icEEG) studies have shown its link to the EZ and predictive value for surgical outcome in these patients. Here, we propose a new noninvasive method based on magnetoencephalography (MEG) and high-density (HD-EEG) data that estimates FC metrics at the source level through an "implantation" of virtual sensors (VSs). We analyzed MEG, HD-EEG, and icEEG data from eight children with MRE who underwent surgery having good outcome and performed source localization (*beamformer*) on noninvasive data to build VSs at the icEEG electrode locations. We analyzed data with and without Interictal Epileptiform Discharges (IEDs) in different frequency bands, and computed the following FC matrices: Amplitude Envelope Correlation (AEC), Correlation (CORR), and Phase Locking Value (PLV). Each matrix was used to generate a graph using Minimum Spanning Tree (MST), and for each node (i.e., each sensor) we computed four centrality measures: betweenness, closeness, degree, and eigenvector. We tested the reliability of VSs measures with respect to icEEG (regarded as *benchmark*) via linear correlation, and compared FC values inside vs. outside resection. We observed higher FC inside than outside resection (p<0.05) for AEC [alpha (8-12 Hz), beta (12-30 Hz), and broadband (1-50 Hz)] on data with IEDs and AEC theta (4-8 Hz) on data without IEDs for icEEG, AEC broadband (1-50 Hz) on data without IEDs for MEG-VSs, as well as for all centrality measures of icEEG and MEG/HD-EEG-VSs. Additionally, icEEG and VSs metrics presented high correlation (0.6-0.9, p<0.05). Our data support the notion that the proposed method can potentially replicate the icEEG ability to map the epileptogenic network in children with MRE.**

Clinical Relevance — **The estimation of FC with noninvasive techniques, such as MEG and HD-EEG, via VSs is a promising tool that would help the presurgical evaluation by delineating the EZ without waiting for a seizure to occur, and potentially improve the surgical outcome of patients with MRE undergoing surgery.**

Corresponding author: christos.papadelis@cookchildrens.org.
L. Corona is from the Department of Bioengineering, University of Texas at Arlington, Arlington, TX, USA (lxc2412@mavs.uta.edu).
L. Corona and C. Papadelis are from Jane and John Justin Neurosciences Center, Cook Children's Health Care System. Fort Worth, TX, USA.
E. Tamilia and C. Papadelis are from Laboratory of Children's Brain Dynamics, Division of Newborn Medicine, Boston Children's Hospital, Harvard Medical School, Boston, MA, USA (eleonora.tamilia@childrens.harvard.edu).
S.M. Stufflebeam is from Athinoula Martinos Center for Biomedical Imaging, Massachusetts General Hospital, Harvard Medical School, Boston, MA, USA (smstufflebeam@mgh.harvard.edu).
P.L. Pearl, C. Papadelis, and J.R. Madsen are from Department of Neurology, Boston Children's Hospital, Harvard Medical School, Boston, MA, USA ({phillip.pearl, joseph.madsen}@childrens.harvard.edu).
C. Papadelis is from School of Medicine, Texas Christian University and University of North Texas Health Science Center, Fort Worth, TX, USA.

I. Introduction

For children with medically refractory epilepsy (MRE), resective surgery is the best option to achieve seizure freedom. If performed early in life, neurosurgery can improve the patient's quality of life [1]. A successful outcome depends on the localization of the epileptogenic zone (EZ), the brain area that is indispensable for the generation of seizures, and its relationship to eloquent areas. The unavailability of methods to directly measure the EZ implicates an imprecise estimation of its location and extent, through the use of noninvasive presurgical tests [2]. When those tests are inconclusive, invasive intracranial electroencephalography (icEEG) is performed, as it is considered the *benchmark* to delineate the seizure onset zone (SOZ), the most logical estimator of the EZ [3]. However, icEEG presents several limitations due to its invasiveness [4], and the implantation of icEEG electrodes is restricted to limited brain areas, leaving others areas unexplored. Thus, noninvasive biomarkers that can identify the EZ are needed to improve the surgical outcome of patients with MRE.

Here, we propose an innovative method based on Functional Connectivity (FC) that quantifies statistical dependencies among remote neurophysiological events in the brain networks. Moreover, we combine FC and graph theory concepts to evaluate how brain areas can be functionally connected in relation to the EZ, with the hypothesis that increases of FC are linked to the EZ, while decreases of FC are seen in distal brain regions [5], [6]. We validated our method by analyzing invasive and noninvasive (MEG and HD-EEG) data of children with MRE, classified as good outcome after surgery, and computed source localization (via *beamformer*) on MEG and HD-EEG to build virtual sensors (VSs) at the same icEEG locations. This noninvasive approach shows how FC computed at the source level (VSs) can provide spatial information of the epileptogenic tissue with comparable precision to the *benchmark* technique (i.e., icEEG). The proposed FC analysis may contribute to the presurgical evaluation of children with MRE since it can help identify the EZ and predict surgical outcome noninvasively, even in the absence of visually noticeable epileptic activity.

II. Methodology

A. Patient cohort

We retrospectively analyzed eight children (five females, age: 12.5 ± 4.72 years) with MRE who underwent epilepsy surgery at Boston Children's Hospital (BCH) between 2011 and 2016 (**Table I**). The inclusion criteria that each patient met in order to be included were the following: (i) long-term monitoring

TABLE I: PATIENT'S INFORMATION

Patient #	Age	Sex	icEEG [#]	Side	Etiology	Res.Vol [cm^3]
1	10	M	ECoG [80]	R	Unknown	13.09
2	6	F	sEEG [90]	L	FCD (T)	13.70
3	10	F	ECoG, sEEG [144+10]	R	DNET (M, Fr)	55.92
4	13	F	ECoG [72]	L	Unknown (T)	18.66
5	17	M	ECoG, sEEG [72+20]	L	N (T)	38.54
6	8	F	ECoG, sEEG [80+20]	R	Unknown	23.71
7	18	M	ECoG [64]	L	FCD (M, T)	32.39
8	18	F	ECoG [88]	L	FCD (Fr)	26.79

M: Male, F: Female, R: Right, L: Left, DNET: Dysembryoplastic Neuroepithelial Tumor, FCD: Focal Cortical Dysplasia, N: Neoplasm, Fr: Frontal, M: Mesial, P: Parietal, T: Temporal.

with icEEG (i.e., grids, strips, and/or depth electrodes); (ii) simultaneous MEG (306 sensors) and HD-EEG (72 channels) recordings, (iii) availability of pre-surgical MRI, post-implantation computerized tomography (CT), and post-operative MRI; (iv) accurate information regarding the resection, and (v) surgical outcome available at least at one year after surgery. Surgical outcomes were evaluated using the Engel's scale (>1 year of post-surgical follow-up), and patients were considered as good outcome when the Engel score was equal to 1. The protocol was approved by BCH Institutional Review Board (IRB-P00022114).

B. Simultaneous HD-EEG and MEG recordings

We performed simultaneous MEG and HD-EEG at the MEG Core Laboratory of Athinoula Martinos Center for Biomedical Imaging (Charlestown, MA). MEG recordings were obtained in a three-layer magnetically shielded room with a 306-channel whole-head MEG system (VectorView, Elekta Neuromag, Helsinki, Finland) characterized by 204 planar gradiometers and 102 magnetometers over 102 locations; HD-EEG recordings were obtained using a 70-channel electrode cap (EASYCAP, Herrsching, Germany) (plus two electrodes covering the low temporal areas at T1 and T2), by positioning the electrodes according to the conventional 10-10 system. Data were acquired with a sampling frequency of 600, 1000, or 2000 Hz.

C. Long-term intracranial EEG recordings

Since noninvasive neuroimaging methods do not always provide accurate information on the EZ, icEEG long-term monitoring (Phase II of the presurgical evaluation) is essential for a better delineation of the epileptic focus and/or the eloquent brain regions. For this study, icEEG was recorded with subdural grids and strips with 2.3 mm of diameter and 10 mm of distance between each one (Ad-Tech., USA), and/or depth electrodes consisted of 10 linearly arranged contacts with 1.1 mm of diameter and 3-5 mm of inter-distance (Ad-Tech., USA) by using XLTEK NeuroWorks (Natus Inc., USA). Data were acquired with a 600, 1000, or 2000 Hz sampling rate. For each patient, the location, number, and type (grids, strips, or depths) of electrodes were prospectively decided as part of patient's surgical plan, which was established by the epilepsy surgical team independently from this study.

D. Identification of each icEEG electrode location

Anatomical MRI scans were acquired before and after surgical resection with magnetization-prepared rapid acquisition gradient-echo sequences (MPRAGE; TE = 1.74 ms, TR = 2, 520 ms, voxel size = 1 × 1 × 1 mm^3) using a high-resolution 3T scanner (TIM TRIO, Siemens AG, Erlangen, Germany). After implantation, Computed Tomography (CT) scans (voxel size = 0.5 × 0.5 × 0.5 mm^3) were performed to obtain the actual locations of icEEG electrodes. Therefore, we determined the anatomical locations of both subdural and depth electrodes by co-registering the post-implantation CT with the pre-operative MRI, using *Brainstorm* [7]. The exact electrode location was defined visually based on the intensity on the co-registered CT-MRI image, and mapped on the three-dimensional model of the patient's cortical surface reconstructed from the preoperative MRI using *FreeSurfer* [8]. To account for brain shift that occurs after electrocorticographic implantation, subdural electrodes were projected onto the cortical surface. Moreover, when both subdural and depth electrodes were implanted, depth electrodes were adjusted to compensate for brain shift [9].

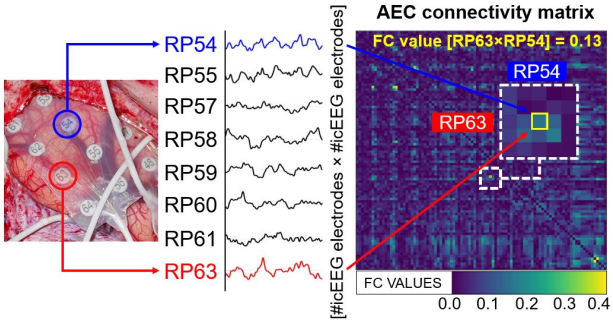

Fig. 1: FC estimates from icEEG. Pairwise FC matrices are estimated for each patient from icEEG. Diagonal elements of the matrix represent the connectivity of each node with itself (containing only zero values); off-diagonal elements of the connectivity matrix represent connectivity between pairs of distinct channels (in this case, icEEG electrodes).

E. VSs reconstruction: forward and inverse method

One of the objectives of this study is to investigate whether FC metrics estimated at the source level from noninvasive methods (MEG/HD-EEG) is comparable with those estimated invasively (icEEG). Firstly, we solved the forward problem by extracting the cortical surfaces from the patient's pre-operative MRI (through *FreeSurfer*), and constructing a realistic head model using *OpenMEEG* software [10]. The realistic boundary elementary model (BEM) was created using a three-layer geometric head model, consisting of the scalp, inner skull, and outer skull, for both MEG and HD-EEG recordings. The source space included the entire brain volume. Secondly, we solved the inverse problem using the linearly constrained minimum variance (LCMV) beamformer [11] in order to localize the underlying neural generators. Data covariance was computed on artifact-free portions selected from MEG and HD-EEG recordings filtered between 1 and 50 Hz, and an identity matrix was used as noise covariance.

The neural activity of each brain location was reconstructed with VSs placed at the same locations where the icEEG electrodes were implanted during Phase II, using the output of the beamformer analysis. Non-overlapping regions of interest (ROIs) were defined for each icEEG electrode and included all the closest volume points surrounding the center of each electrode: 5 mm and 10 mm for depth and subdural electrodes, respectively [9]. Finally, we reconstructed VSs time-series for MEG (MEG-VSs) and HD-EEG (HD-EEG-VSs) separately by computing for each VS its mean activation (mean across volume points) [9].

F. Functional Connectivity Analysis

For each patient, icEEG and the reconstructed VSs time-series (MEG-VSs and HD-EEG-VSs) were pre-processed and filtered between 1 and 50 Hz. Data were then classified as (i) with IEDs (3-s segments containing frequent interictal spikes), and (ii) without IEDs (3-s segments containing minimal interictal spikes or no spikes at all). To this purpose, for each signal (i.e., icEEG, MEG-VSs, HD-EEG-VSs), we visually selected and then analyzed one-minute (20 epochs of 3 s) of each type of activity. The functional organization of anatomically separated brain regions was explored using the following FC methods: (i) Amplitude Envelope Correlation (AEC), (ii) Correlation (CORR), and (iii) Phase Locking Value (PLV). We selected these methods to capture different characteristics of iteration among brain signals across functionally connected regions by focusing on the similarity between two signals in the time domain (CORR), the amplitude correlation (AEC), and the instantaneous phase difference (PLV), respectively [12]. These three methods were computed for the following frequency bands: delta (1-4 Hz), theta (4-8 Hz), alpha (8-12 Hz), beta (12-30 Hz), gamma (30-50 Hz), and a broadband of frequencies (1-50 Hz). Thus, for each patient, we computed three FC matrices (AEC, CORR, PLV) for each epoch and each type of data (IEDs vs. without IEDs) using *Brainstorm*. The connectivity matrix (**Fig. 1**), characterized by N×N nodes, describes the pairwise connectivity between all nodes of the network [13], which here correspond to icEEG electrodes (for the invasive analysis) and to VSs (for the noninvasive analyses). Finally, for each patient we obtained three averaged FC matrices (i.e., AEC, CORR, PLV), separately for both data with and without IEDs, after averaging across epochs. These FC matrices were used to investigate the centrality of each brain region (corresponding to each sensor) within the network [6], using the graph theory.

G. Graph Theory Analysis

Each average FC matrix was used to represent the brain of each patient as a graph consisting of a set of *nodes*, corresponded to each row and column of the matrix (equal to icEEG electrodes and VSs), and undirected weighted *edges*, corresponded to the inverted FC values [14]. For each patient, we mapped a subnetwork, known as the Minimum Spanning Tree (MST) [15], based on each FC matrix (i.e., AEC, CORR and PLV, separately for data with and without IEDs) of icEEG, MEG-VSs and HD-EEG-VSs signals (**Fig. 2**), using MATLAB®. Then, we estimated the importance of each electrode (node) within the network of each patient by computing four centrality measures from each MST [16]: (i) *betweenness*: number of times a node acts as a "bridge" along the shortest path between two other nodes; (ii) *closeness*: average length of the shortest path between the node and all other nodes in the graph; (iii) *degree*: number of links connected to a node; and (iv) *eigenvector*: measure of the influence of a node in a network.

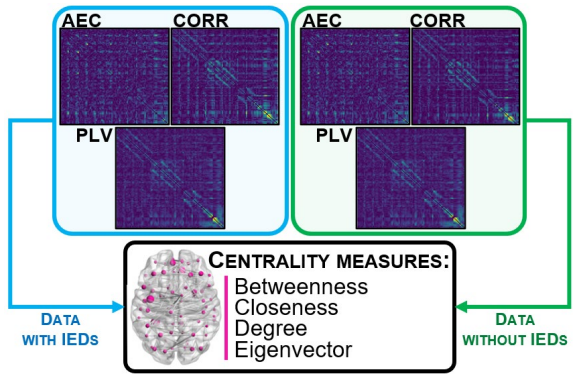

Fig. 2: Graph analysis computed on each FC matrix. On each averaged FC matrix (AEC, CORR, PLV), computed for data with IEDs and without IEDs separately, we represented the brain of each patient as a graph by using the MST and computing its centrality measures to estimate the importance of each node (sensor) within the network.

H. Resected vs. non-resected areas

We defined the boundaries of the resected area by co-registering the pre-operative and post-operative MRIs via *Brainstorm*. For each icEEG electrode and VSs, we computed their distance from resection as the Euclidian distance of their center from the closest resection margin [17]. Then, we defined as resected the sensors (icEEG and VSs) that have a distance $\leq$ 10 mm from resection. This differentiation between the two zones (resected vs. non-resected area) helped us to associate our FC and centrality measures with the EZ, which we could assume to correspond to the resection, since the patients were seizure-free after surgery (good surgical outcome).

I. Statistical Analysis

We used a Wilcoxon signed-rank test to compare the FC and centrality measures, estimated from icEEG and VSs, between inside and outside resection. Statistical analysis was performed in MATLAB®, and we considered statistical significance for $p < 0.05$. Further, we used Spearman's rank correlation to assess the correlation of FC and centrality measures between icEEG and VSs, separately for resected and non-resected areas.

III. Results

A. Invasive (icEEG) findings

We observed that icEEG FC were increased inside resection compared to outside, with a $p = 0.0078$ obtained for all the following measures: AEC [for alpha, beta, and broadband bands] on data with IEDs, and AEC theta on data without IEDs. Using graph analysis, we observed that all centrality measures (i.e., betweenness, closeness, degree, and eigenvector), estimated from both AEC and PLV methods on data with and without IEDs, were higher inside than outside resection ($p < 0.05$).

B. *Noninvasive findings (MEG-VSs and HD-EEG-VSs)*

From MEG-VSs analysis, we found increased AEC inside compared to outside resection ($p = 0.0156$), for the broadband data without IEDs. On the other hand, HD-EEG-VSs analysis did not show statistical significance for any FC metrics. From the graph analysis, we observed higher connectivity within resection compared to outside ($p < 0.05$) from both MEG-VSs and HD-EEG-VSs analyses. HD-EEG-VSs analysis showed significant differences for all centrality measures (i.e., betweenness, closeness, degree, and eigenvector), obtained from both CORR and PLV methods on data with and without IEDs; MEG-VSs analysis showed significant differences for betweenness, closeness, and degree, estimated from both AEC and PLV methods on data without IEDs.

C. *Invasive vs. noninvasive findings*

We showed the association of two centrality measures (i.e., AEC closeness theta and PLV betweenness theta on data without IEDs), obtained from both icEEG and MEG-VSs, with the EZ (**Fig. 3**). Both these metrics showed higher values inside resection than outside ($p < 0.05$) for icEEG and MEG-VSs data, and a similar trend was obtained for HD-EEG-VSs without reaching a statistical significance. Further, we found that several icEEG FC and graph metrics correlated significantly with the same metrics estimated via VSs, both inside and outside resection, with a Spearman's *rho* comprised between 0.6 and 0.9 ($p < 0.05$).

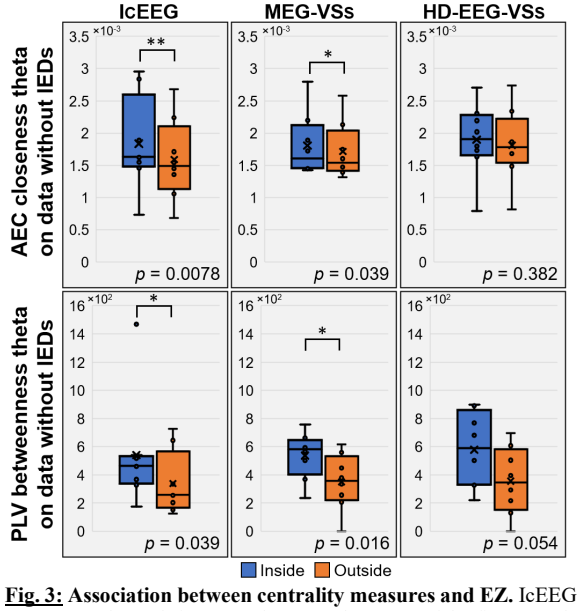

Fig. 3: Association between centrality measures and EZ. IcEEG and MEG-VSs showed, for AEC closeness theta (top of the figure) and PLV betweenness theta (bottom of the figure), higher connectivity inside than outside resection on data without IEDs. A similar trend was observed for HD-EEG-VSs without obtaining statistical significance.

IV. Conclusions

In this study, we propose a new noninvasive method, based on MEG and HD-EEG, that estimates FC metrics at the source level through an "implantation" of virtual sensors (VSs) in children with MRE undergoing presurgical evaluation. Our retrospective data support our hypothesis that increased FC is linked to the EZ, since we showed that, for patients with good surgical outcome (regarded as *benchmark* to identify the EZ correctly), higher FC values were found inside compared to outside resection. As well, graph analysis suggests that highly central nodes (*hubs*) are located inside resection zone for both icEEG and VSs analyses, since higher centrality values were seen there compared to outside. Our results confirm that FC metrics estimated at the source level from noninvasive data, by reconstructing VSs (*beamformer*) at the icEEG locations, provide similar findings to those obtained invasively. This methodological limitation of our study could open up new possibilities to build VSs not only in specific positions but in the entire cortex, overcoming spatial limitations of icEEG. Further, several findings were obtained on data with IEDs as well as without IEDs: this could provide prognostic correlates useful for treating pediatric epilepsy even in the absence of visually noticeable epileptic activity in MEG/HD-EEG recordings. Our proposed method could help the presurgical evaluation of children with MRE by estimating the EZ without waiting for a seizure to occur, and potentially improve surgical outcomes.

Acknowledgment

This work was supported by the National Institute of Neurological Disorders & Stroke 454 (RO1NS104116-01A1, PI: C. Papadelis; 1R21NS101373-01A1, PIs: C. Papadelis & S. Stufflebeam), and Cook Children's Health Foundation.

References

[1] B. McCoy and S. R. Benbadis, "Approach to refractory childhood seizures," *Therapy*, vol. 7, no. 5, pp. 497–506, 2010.
[2] F. Rosenow and H. Luders, "Presurgical evaluation of epilepsy," pp. 1683–1700, 2001.
[3] E. Tamilia, J. R. Madsen, P. E. Grant, P. L. Pearl, and C. Papadelis, "Current and emerging potential of magnetoencephalography in the detection and localization of high-frequency oscillations in epilepsy," *Front. Neurol.*, vol. 8, no. JAN, 2017.
[4] W. J. Hader *et al.*, "Complications of epilepsy surgery - A systematic review of focal surgical resections and invasive EEG monitoring," *Epilepsia*, vol. 54, no. 5, pp. 840–847, 2013.
[5] P. Shah *et al.*, "High interictal connectivity within the resection zone is associated with favorable post-surgical outcomes in focal epilepsy patients," *NeuroImage Clin.*, vol. 23, no. April, p. 101908, 2019.
[6] I. A. Nissen *et al.*, "Identifying the epileptogenic zone in interictal resting-state MEG source-space networks," *Epilepsia*, vol. 58, no. 1, pp. 137–148, 2017.
[7] F. Tadel, S. Baillet, J. C. Mosher, D. Pantazis, and R. M. Leahy, "Brainstorm: A user-friendly application for MEG/EEG analysis," *Comput. Intell. Neurosci.*, vol. 2011, 2011.
[8] K. De Macedo Rodrigues *et al.*, "A FreeSurfer-compliant consistent manual segmentation ofinfant brains spanning the 0–2 year age range," *Front. Hum. Neurosci.*, vol. 9, no. FEB, pp. 1–12, 2015.
[9] E. Tamilia *et al.*, "Noninvasive Mapping of Ripple Onset Predicts Outcome in Epilepsy Surgery," pp. 1–15, 2021.
[10] A. Gramfort, T. Papadopoulo, E. Olivi, and M. Clerc, "OpenMEEG: Opensource software for quasistatic bioelectromagnetics," *Biomed. Eng. Online*, vol. 9, pp. 1–20, 2010.
[11] B. D. Van Veen, W. Van Drongelen, M. Yuchtman, and A. Suzuki, "Localization of brain electrical activity via linearly constrained minimum variance spatial filtering," *IEEE Trans. Biomed. Eng.*, vol. 44, no. 9, pp. 867–880, 1997.
[12] B. He *et al.*, "Electrophysiological Brain Connectivity: Theory and Implementation," *IEEE Trans. Biomed. Eng.*, vol. 66, no. 7, pp. 2115–2137, 2019.
[13] A. Fornito, A. Zalesky, and E. T. Bullmore, *Fundamentals of Brain Network Analysis*. Elsevier Inc., 2016.
[14] E. L. Juárez-Martinez *et al.*, "Virtual localization of the seizure onset zone: Using non-invasive MEG virtual electrodes at stereo-EEG electrode locations in refractory epilepsy patients," *NeuroImage Clin.*, vol. 19, no. March, pp. 758–766, 2018.
[15] E. Van Dellen *et al.*, "Epilepsy surgery outcome and functional network alterations in longitudinal MEG: A minimum spanning tree analysis," *Neuroimage*, vol. 86, pp. 354–363, 2014.
[16] F. V. Farahani, W. Karwowski, and N. R. Lighthall, "Application of graph theory for identifying connectivity patterns in human brain networks: A systematic review," *Front. Neurosci.*, vol. 13, no. JUN, pp. 1–27, 2019.
[17] M. Alhilani *et al.*, "Ictal and interictal source imaging on intracranial EEG predicts epilepsy surgery outcome in children with focal cortical dysplasia," *Clin. Neurophysiol.*, vol. 131, no. 3, pp. 734–743, 2020.